1,2-propanediol as a surrogate molecule of glycerol for mechanistic studies of selective hydrodeoxygenation reactions over Mo_2C and Cu/Mo_2C surfaces

Zhexi Lin, [†] *Weiming Wan* [†] *and Jingguang G. Chen* *[,†]

[†]Department of Chemical Engineering, Columbia University, 500 W. 120th Street, New York, NY, 10027, United States. *E-mail: jgchen@columbia.edu

KEYWORDS: Carbides, Glycerol, 1,2-propanediol, Hydrodeoxygenation, Mechanistic Studies

ABSTRACT

The upgrading of glycerol, a by-product from biodiesel production, is important for developing more sustainable biomass conversion technologies. Nonetheless, the low vapor pressure and structural complexity of glycerol limit mechanistic studies of gas-phase reactions on model surfaces and powder catalysts. In this work, we demonstrate the feasibility of using 1,2-propanediol (PDO) as a surrogate compound for the mechanistic study of glycerol over Mo_2C and Cu/Mo_2C surfaces. The results show that glycerol and 1,2-PDO undergo similar reaction pathways on both the Mo and Cu sites, suggesting that 1,2-PDO could be used as a higher vapor pressure surrogate to glycerol for gas-phase mechanistic studies.

Introduction

The production of fuels and chemicals from renewable biomass resources has drawn significant attention in recent years.[1–8] Biodiesel production is a promising approach of utilizing biomass to help reduce the environmental impact from fossil fuels.[9] Biodiesel is produced mainly via the transesterification reaction of triglyceride with methanol, in which glycerol is formed as a by-product.[10] As the biodiesel production grows rapidly, there is a large surplus of glycerol, which is generally considered as a platform molecule that can be upgraded into many value-added chemicals. Glycerol can be converted using enzymatic and chemical methods. The enzymatic transformations of glycerol have shown promise in producing specialty chemicals, such as 2,3-butanediol,[11,12] or intermediates that can be further upgraded by chemical methods, such as 3-hydroxypropanal.[13–15] On the other hand, chemical conversions of glycerol provide added capability for upgrading glycerol via a variety of pathways. Typical chemical conversion pathways for glycerol include selective oxidation,[16,17] etherification,[18,19] acetylation,[20,21] reforming,[22,23] dehydration,[24,25] and selective hydrogenolysis/hydrodeoxygenation.[26,27] Among these approaches, selective hydrodeoxygenation (HDO) is a particularly interesting approach, in which glycerol can be upgraded into various specialty chemicals, such as allyl alcohol, acetol and propanal. It is generally accepted that Cu-based catalysts are very selective in converting glycerol into 1,2-PDO. In this process glycerol is typically first catalyzed by acid sites into the acetol intermediate, which is then hydrogenated by the surface Cu sites to form 1,2-PDO.[28–35] Under ultra-high vacuum (UHV) conditions, due to low hydrogen partial pressure, the final product of glycerol HDO reaction over Cu sites should likely be acetol instead. Wan et al. have demonstrated that the bond-breaking sequences of glycerol can be tuned by controlling the coverage of Cu modifiers on a molybdenum carbide (Mo_2C) surface , in which the oxygen

binding energy of the surface plays an important role in determining the final HDO products.[36] Despite the interesting results on the Cu/Mo_2C surfaces, the low vapor pressure and high viscosity of glycerol make it particularly difficult to conduct gas-phase mechanistic studies on both model surfaces and the corresponding powder catalysts. The elucidation of reaction mechanism and activation barriers by *ab initio* computation is also expensive due to the structural complexity resulting from the presence of three -OH groups in glycerol. To date, only very few fundamental studies for glycerol have been done on model surfaces using surface science techniques, mainly due to the experimental difficulties in introducing pure glycerol into ultra-high vacuum (UHV) systems.[36,37]

To this end, this work compares the reaction pathways of glycerol, 1,2- and 1,3-PDO, in an attempt to evaluate whether the diols can serve as model compounds for the study of gas-phase glycerol reaction under UHV conditions. 1,2- and 1,3-PDO are chosen because their structures are similar to that of glycerol and that both diols contain one less -OH functional group than glycerol. The higher vapor pressures of these diols ease the difficulty in introducing reactant into the UHV chamber and also make it potentially possible to carry out gas-phase reactor evaluation on the corresponding powder catalysts. Temperature-programmed desorption (TPD) experiments were performed to probe the gas-phase products from the reactions, and high-resolution electron energy loss spectroscopy (HREELS) measurements were conducted to identify the surface reaction intermediates. The results show that 1,2-PDO and glycerol undergo similar reaction pathways via similar intermediates on the Mo and Cu sites of the Cu/Mo_2C surfaces, suggesting the feasibility of using 1,2-PDO as a surrogate molecule for further mechanistic studies of glycerol.

Results and Discussion

The Mo_2C surface was synthesized by following a previously published procedure[38,39] and the details can be found in the Supporting Information. Briefly, a Mo(110) single crystal was exposed to ethylene, followed by annealing to achieve a Mo-terminated Mo_2C surface with a p(4x4) LEED pattern. Cu was deposited onto Mo_2C using the physical vapor deposition (PVD) method. Figure 1 shows the TPD spectra of propylene after dosing glycerol, 1,2- and 1,3-PDO on the Mo_2C and 0.8ML Cu/Mo_2C surfaces. The sharp peaks at 263K, 211K and 229K represent the cracking fragments of desorbed glycerol, 1,2- and 1,3-PDO, respectively. For glycerol and 1,2-PDO on Mo_2C (Figure 1(a)), the broad peaks between 250K and 700K are contributed from the desorption of propylene, which is a product from glycerol and 1,2-PDO from the unselective HDO. One should note that for 1,3-PDO, there is also a broad peak between 350K and 700K. This peak is also from the desorption of propylene but has a different peak shape than those of glycerol and 1,2-PDO. Since there the m/z=57 peak is not observed from the reactions of all three molecules on Mo_2C (Figure S5), allyl alcohol is not formed and only propylene is produced on Mo_2C. The similar peak shapes and desorption temperatures of propylene from 1,2-PDO and glycerol suggest that these two molecules likely undergo similar C-O bond scission steps to produce propylene. As Cu coverage increases to 0.8ML (Figure 1(b)), the propylene peaks from all three molecules decrease, which is consistent with a previous study[36] that propylene is produced on the Mo site. For glycerol on 0.8 ML Cu/Mo_2C, on top of the broad propylene peak there is another sharp peak at 363K, which is contributed from allyl alcohol/propanal formation that only occurs on the Cu/Mo_2C interface.[36] The propylene spectra from the 0.3ML Cu/Mo_2C surface are shown in Figure S1.

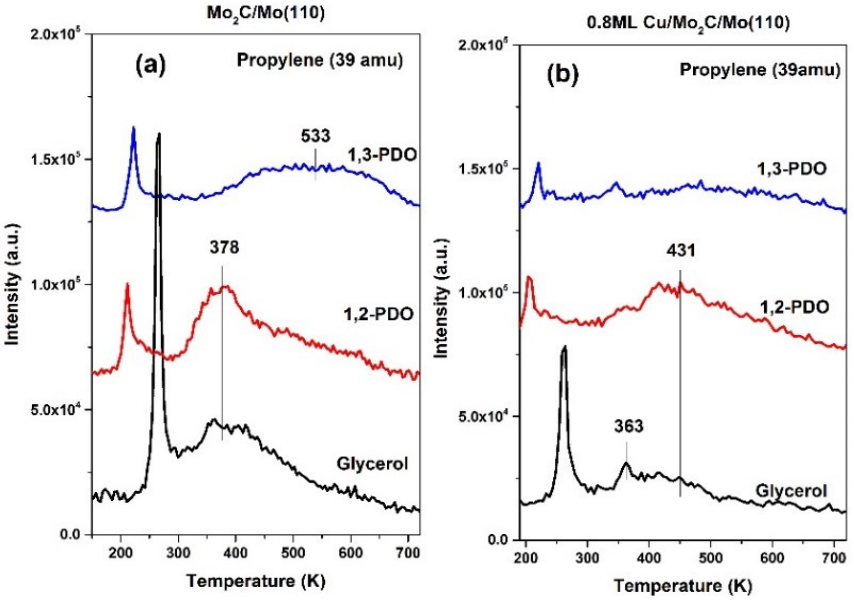

Figure 1. TPD spectra of propylene following an exposure of 4L glycerol, 1,2-PDO and 1,3-PDO over hydrogen pre-dosed (a) Mo_2C and (b) 0.8ML Cu/Mo_2C.

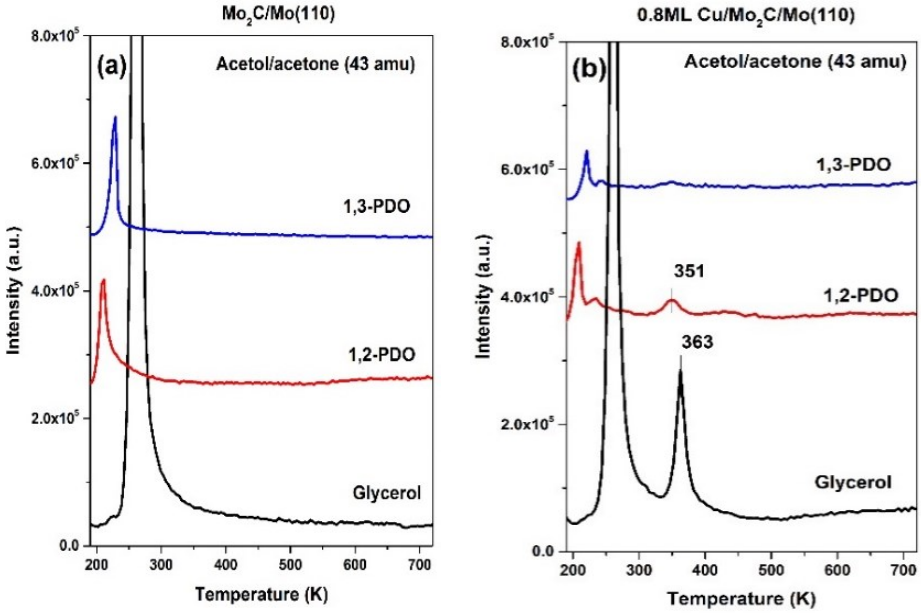

Figure 2. TPD spectra of acetol/acetone following an exposure of 4L glycerol, 1,2-PDO and 1,3-PDO over hydrogen pre-dosed (a) Mo_2C and (b) 0.8ML Cu/Mo_2C.

Figure 2 shows the desorption of acetol and acetone (43 amu) produced from glycerol and 1,2-PDO. One should note that both acetol and acetone have a common cracking fragment of 43 amu. Additional fragments for acetol (74 amu) and acetone (58 amu) are shown in the

supporting information (Figure S2 and Figure S3) to confirm the formation of such products. Similar to the 39 amu spectra in Figure 1, the sharp peaks at 263K, 211K and 229K in Figure 2 are from the cracking fragment of glycerol, 1,2- and 1,3-PDO, respectively. On Mo_2C (Figure 2(a)), there are no additional peaks besides the cracking fragments of the reactant molecules. On the 0.8 ML Cu/Mo_2C surface (Figure 2(b)) the peaks around 363K and 351K are observed for glycerol and 1,2-PDO, respectively. The TPD spectra from 0.3ML Cu/Mo_2C are shown in Figure S1. Since the amount of acetol and acetone produced from glycerol and 1,2-PDO increases as the Cu coverage increases, these products are likely formed on the Cu site of the Cu/Mo2C surfaces, rather than the Cu/Mo_2C interfacial site. The production of acetol from glycerol and acetone from 1,2-PDO indicates that glycerol and 1,2-PDO undergo similar bond breaking sequence on the Cu site, which selectively cleaves the primary C-O bond and dehydrogenates the secondary –OH group. On the other hand, no 43 amu peak is produced from 1,3-PDO. Instead, 29 amu and 58 amu peaks at 341K were detected after dosing 1,3-PDO. As the Cu coverage increases, the peak areas of 29 amu and 58 amu also increase, suggesting that propanal is produced from 1,3-PDO on the Cu sites (Figure S4 and S3). The reaction pathways of glycerol, 1,2- and 1,3-PDO are summarized in Scheme 1. Compared to the Mo site that cleaves all the C-O bonds of C3 polyols, the Cu site can only cleave one C-O bond, likely due to the lower oxygen binding energy of Cu. Note that since the Cu modifier may agglomerate during the deposition process at 600K, the surfaces with Cu coverage greater than 1ML are not discussed in this work. The quantification results of all the C3 products from glycerol, 1,2- and 1,3-PDO on the Mo_2C and 0.8ML Cu/Mo_2C surfaces are shown in Table 1, while those of the 0.3ML Cu/Mo_2C surface are shown in Table S1.

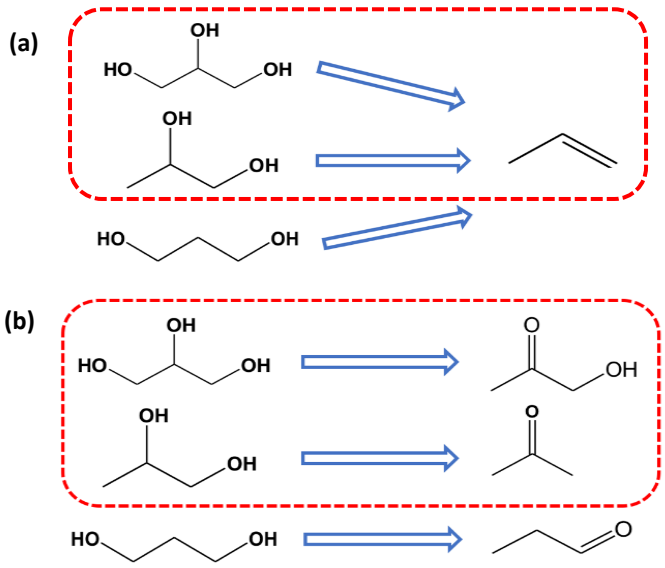

Scheme 1. Reaction pathways of glycerol, 1,2- and 1,3-PDO over (a) Mo site and (b) Cu site on Mo_2C and Cu/Mo_2C surfaces.

Table 1. Activity (molecules per metal atom) of C3 products from glycerol and diols over corresponding surfaces.

	θ_{Cu} (ML)	Propylene	Acetol	Acetone	Allyl alcohol /Propanal	Total
Glycerol	0	0.061	0.000	0.000	0.000	0.061
	0.8	0.021	0.051	0.000	0.007	0.079
1,2-PDO	0	0.040	0.000	0.000	0.000	0.040
	0.8	0.026	0.000	0.006	0.000	0.032
1,3-PDO	0	0.030	0.000	0.000	0.000	0.030
	0.8	0.013	0.000	0.000	0.007	0.020

θ_{Cu}: coverage of copper. ML: monolayer

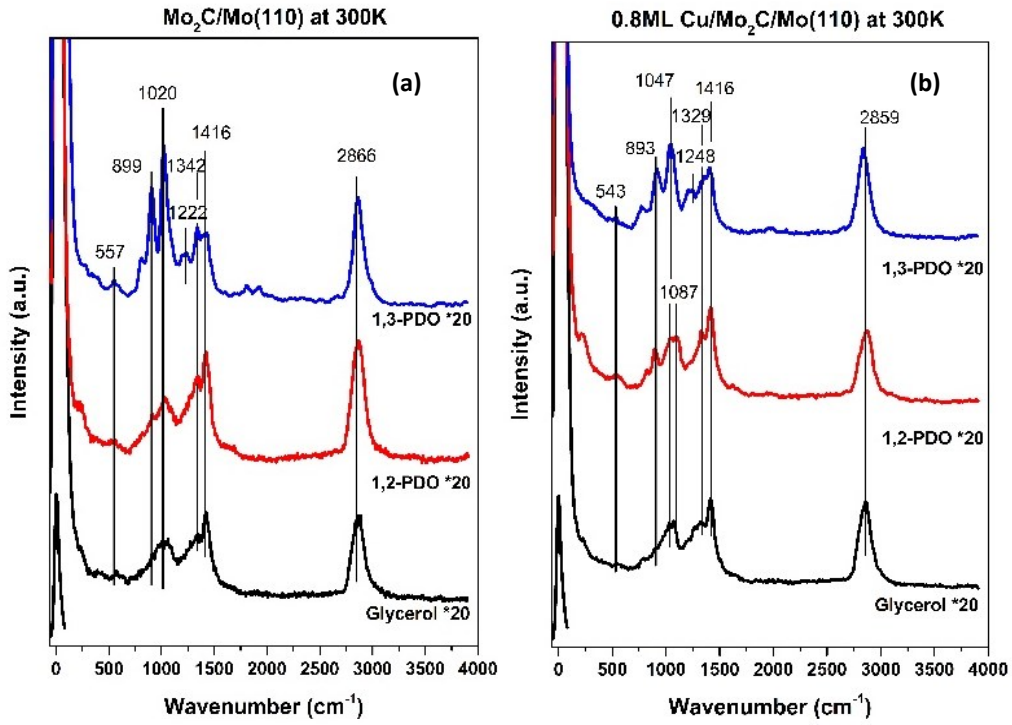

Figure 3. Comparison of HREEL spectra after an exposure of 4L of glycerol, 1,2-and 1,3-PDO over hydrogen pre-dosed (a) Mo_2C and (b) 0.8ML Cu/Mo_2C at 300K.

The HREELS measurements were performed to compare the surface reaction intermediates of glycerol and 1,2- and 1,3-PDO. The vibrational mode assignments are summarized in Table 2. Shown in Figure 3 are the HREEL spectra of glycerol, 1,2- and 1,3-PDO on the Mo_2C and 0.8ML Cu/Mo_2C surfaces at 300K. In general, the spectra of glycerol and 1,2-PDO are very similar on both the Mo_2C and 0.8ML Cu/Mo_2C surfaces, indicating that both molecules likely produce similar intermediates. The spectra for molecularly adsorbed glycerol, 1,2- and 1,3-PDO are shown in Figure S7 in the Supporting Information. Even though the spectra of molecularly adsorbed 1,2-PDO and glycerol appear slightly different, the spectra of both molecules become very similar when temperature is increased to 300K and above. In contrast, the 1,3-PDO spectra on both surfaces are quite different than the other two molecules, especially in the region between 890 cm^{-1} and 1100 cm^{-1}. The $\rho_r(CH_2)$ mode of 1,3-PDO on both Mo_2C (899 cm^{-1}) and 0.8ML Cu/Mo_2C (893 cm^{-1}) are more intense than those of glycerol and 1,2-PDO on the corresponding surfaces, consistent with the fact that there are more -CH_2 groups in 1,3-PDO than in glycerol and 1,2-PDO. Furthermore, on Mo_2C, the ν(CO) mode at 1020 cm^{-1} of 1,3-PDO is more intense than those of 1,2-PDO and glycerol, indicating that the C-O bond of 1,3-PDO is better preserved than those of glycerol and 1,2-PDO, which is consistent with the TPD observations that propylene is formed at higher onset temperature from 1,3-PDO (350K) than from glycerol (210 K) or 1,2-PDO (300K). Additionally, on the 0.8ML Cu/Mo_2C surface, there are two peaks at 1047 cm^{-1} and 1087 cm^{-1} that represent the ν(CO) mode for 1,2-PDO and glycerol, respectively. These two peaks correspond to the two types of C-O bonds in 1,2-PDO and glycerol (primary and secondary). In comparison, only one peak is observed at 1047 cm^{-1} for 1,3-PDO, consistent with the presence of only one type of C-O bond (primary) in 1,3-PDO. When the surface temperature is further increased to 400K, glycerol and 1,2-PDO still show very

similar spectra on both Mo_2C and 0.8ML Cu/Mo_2C, but the differences between 1,3-PDO and the other two become more significant. (Figure S5)

Table 2. Vibrational mode assignments for glycerol, 1,2- and 1,3-PDO over corresponding surfaces

Mode	Frequency (cm^{-1})			
	Ethylene glycol on $Mo_2C/Mo(110)$[a]	1,2-PDO liquid IR [b]	$Mo_2C/Mo(110)$[c]	0.8ML $Cu/Mo_2C/Mo(110)$ [c]
$\boldsymbol{\nu(MO)}$			557	543
$\boldsymbol{\rho_r(CH_2)}$	879	839	899	893
$\boldsymbol{\nu(CO)}$	1069	1046	1020	1047
$\boldsymbol{\nu(CO)}$		1138		1087
$\boldsymbol{\rho_t(CH_2)}$	1260	1289	1222	1248
$\boldsymbol{\rho_w(CH_2)}$	1360		1342	1329
$\boldsymbol{\delta(CH_2)}$	1441	1455	1416	1416
$\boldsymbol{\nu(CH)}$	2916	2935	2866	2859

δ - deformation, ρ_r - rocking, ν - stretching, ρ_t - torsion, ρ_w - wagging.

[a] ref [40],

[b] ref [41],

[c] This work

Conclusions

In summary, TPD experiments show that glycerol and 1,2-PDO undergo similar bond breaking sequence on the Mo and Cu sites of the Cu/Mo_2C surface. The Mo site tends to cleave all the C-O bond of both molecules to form propylene, while the Cu site breaks the primary C-O

bonds to form acetol and acetone, respectively. The resemblance between the HREEL spectra of 1,2-PDO and glycerol indicates that glycerol and 1,2-PDO likely undergo primary C-O bond scission to form similar intermediates. Overall, these results suggest that 1,2-PDO can potentially be used as a surrogate molecule for glycerol. The higher vapor pressure of 1,2-PDO eases the dosing process in UHV chambers and should allow for gas-phase flow reactor evaluations. The simpler structure of 1,2-PDO should also significantly reduce the computational expense for activation barrier calculations. These will facilitate further mechanistic studies on the C-O bond breaking sequence of glycerol and provide insights into designing more efficient catalysts for the selective HDO of glycerol.

ASSOCIATED CONTENT

Supporting Information.

The following files are available free of charge.

Experimental details, additional quantification results, TPD and HREELS figures (PDF)

AUTHOR INFORMATION

Corresponding Author

*J.G. Chen. Email: jgchen@columbia.edu

Notes

The authors declare no competing financial interest.

ACKNOWLEDGMENT

This article was sponsored by the Catalysis Center for Energy Innovation (CCEI), an Energy Frontier Research Center (EFRC) funded by the U.S. Department of Energy, Office of Basic Energy Sciences under Award Number DE-SC0001004.

REFERENCES

(1) Huber, G. W.; Iborra, S.; Corma, A. Synthesis of Transportation Fuels from Biomass: Chemistry, Catalysts, and Engineering. *Chem. Rev.* **2006**, *106* (9), 4044–4098. https://doi.org/10.1021/cr068360d.

(2) Chheda, J. N.; Huber, G. W.; Dumesic, J. A. Liquid-Phase Catalytic Processing of Biomass-Derived Oxygenated Hydrocarbons to Fuels and Chemicals. *Angew. Chemie - Int. Ed.* **2007**, *46* (38), 7164–7183. https://doi.org/10.1002/anie.200604274.

(3) Wang, H.; Male, J.; Wang, Y. Recent Advances in Hydrotreating of Pyrolysis Bio-Oil and Its Oxygen-Containing Model Compounds. *ACS Catal.* **2013**, *3* (5), 1047–1070. https://doi.org/10.1021/cs400069z.

(4) Jiang, Z.; Wan, W.; Lin, Z.; Xie, J.; Chen, J. G. Understanding the Role of M / Pt (111) (M = Fe , Co , Ni , Cu) Bimetallic Surfaces for Selective Hydrodeoxygenation of Furfural. *ACS Catal.* **2017**, *7* (9), 5758–5765. https://doi.org/10.1021/acscatal.7b01682.

(5) Wan, W.; Jenness, G. R.; Xiong, K.; Vlachos, D. G.; Chen, J. G. Ring-Opening Reaction of Furfural and Tetrahydrofurfuryl Alcohol on Hydrogen-Predosed Iridium(1 1 1) and Cobalt/Iridium(1 1 1) Surfaces. *ChemCatChem* **2017**, *9* (9), 1701–1707.

https://doi.org/10.1002/cctc.201601646.

(6) Sauter, W.; Bergmann, O. L.; Schröder, U. Hydroxyacetone: A Glycerol-Based Platform for Electrocatalytic Hydrogenation and Hydrodeoxygenation Processes. *ChemSusChem* **2017**, *10* (15), 3105–3110. https://doi.org/10.1002/cssc.201700996.

(7) Robinson, A. M.; Hensley, J. E.; Will Medlin, J. Bifunctional Catalysts for Upgrading of Biomass-Derived Oxygenates: A Review. *ACS Catal.* **2016**, *6* (8), 5026–5043. https://doi.org/10.1021/acscatal.6b00923.

(8) Lin, Z.; Chen, R.; Qu, Z.; Chen, J. G. Hydrodeoxygenation of Biomass-Derived Oxygenates over Metal Carbides: From Model Surfaces to Powder Catalysts. *Green Chem.* **2018**, *20* (12), 2679–2696. https://doi.org/10.1039/C8GC00239H.

(9) Lin, L.; Cunshan, Z.; Vittayapadung, S.; Xiangqian, S.; Mingdong, D. Opportunities and Challenges for Biodiesel Fuel. *Appl. Energy* **2011**, *88* (4), 1020–1031. https://doi.org/10.1016/j.apenergy.2010.09.029.

(10) Okoye, P. U.; Hameed, B. H. Review on Recent Progress in Catalytic Carboxylation and Acetylation of Glycerol as a Byproduct of Biodiesel Production. *Renew. Sustain. Energy Rev.* **2016**, *53*, 558–574. https://doi.org/10.1016/j.rser.2015.08.064.

(11) Ripoll, V.; de Vicente, G.; Morán, B.; Rojas, A.; Segarra, S.; Montesinos, A.; Tortajada, M.; Ramón, D.; Ladero, M.; Santos, V. E. Novel Biocatalysts for Glycerol Conversion into 2,3-Butanediol. *Process Biochem.* **2016**, *51* (6), 740–748. https://doi.org/10.1016/J.PROCBIO.2016.03.006.

(12) Metsoviti, M.; Paramithiotis, S.; Drosinos, E. H.; Galiotou-Panayotou, M.; Nychas, G.-J. E.; Zeng, A.-P.; Papanikolaou, S. Screening of Bacterial Strains Capable of Converting Biodiesel-Derived Raw Glycerol into 1,3-Propanediol, 2,3-Butanediol and Ethanol. *Eng.*

Life Sci. **2012**, *12* (1), 57–68. https://doi.org/10.1002/elsc.201100058.

(13) Toraya, T.; Shirakashi, T.; Kosuga, T.; Fukui, S. Substrate Specificity of Coenzyme B12-Dependent Diol Dehydrase: Glycerol as Both a Good Substrate and a Potent Inactivator. *Biochem. Biophys. Res. Commun.* **1976**, *69* (2), 475–480. https://doi.org/10.1016/0006-291X(76)90546-5.

(14) Foraget, R. G.; Foster, M. A. Glycerol Fermentation in Klebsiella Pneumoniae: Functions of the Coenzyme B12-Dependent Glycerol and Diol Dehydratases. *J. Bacteriol.* **1982**, *149* (2), 413–419.

(15) Abeles, R. H.; Brownstein, A. M.; Randles, C. H. β-Hydroxypropionaldehyde, an Intermediate in the Formation of 1,3-Propanediol by Aerobacter Aerogenes. *Biochim. Biophys. Acta* **1960**, *41* (3), 530–531. https://doi.org/10.1016/0006-3002(60)90054-8.

(16) Carrettin, S.; McMorn, P.; Johnston, P.; Griffin, K.; Hutchings, G. J. Selective Oxidation of Glycerol to Glyceric Acid Using a Gold Catalyst in Aqueous Sodium Hydroxide. *Chem. Commun.* **2002**, No. 7, 696–697. https://doi.org/10.1039/b201112n.

(17) Qi, J.; Xin, L.; Chadderdon, D. J.; Qiu, Y.; Jiang, Y.; Benipal, N.; Liang, C.; Li, W. Electrocatalytic Selective Oxidation of Glycerol to Tartronate on Au/C Anode Catalysts in Anion Exchange Membrane Fuel Cells with Electricity Cogeneration. *Appl. Catal. B Environ.* **2014**, *154–155*, 360–368. https://doi.org/10.1016/j.apcatb.2014.02.040.

(18) Lemos, C. O. T.; Rade, L. L.; Barrozo, M. A. D. S.; Fernandes, L. D.; Cardozo-Filho, L.; Hori, C. E. Optimization of Catalytic Glycerol Etherification with Ethanol in a Continuous Reactor. *Energy and Fuels* **2017**, *31* (5), 5158–5164. https://doi.org/10.1021/acs.energyfuels.7b00194.

(19) Zhou, J.; Wang, Y.; Guo, X.; Mao, J.; Zhang, S. Etherification of Glycerol with Isobutene

on Sulfonated Graphene: Reaction and Separation. *Green Chem.* **2014**, *16* (11), 4669–4679. https://doi.org/10.1039/C4GC01044B.

(20) Troncea, S. B.; Wuttke, S.; Kemnitz, E.; Coman, S. M.; Parvulescu, V. I. Hydroxylated Magnesium Fluorides as Environmentally Friendly Catalysts for Glycerol Acetylation. *Appl. Catal. B Environ.* **2011**, *107* (3–4), 260–267. https://doi.org/10.1016/j.apcatb.2011.07.021.

(21) Kim, I.; Kim, J.; Lee, D. A Comparative Study on Catalytic Properties of Solid Acid Catalysts for Glycerol Acetylation at Low Temperatures. *Appl. Catal. B Environ.* **2014**, *148–149*, 295–303. https://doi.org/10.1016/j.apcatb.2013.11.008.

(22) Karim, A. M.; Howard, C.; Roberts, B.; Kovarik, L.; Zhang, L.; King, D. L.; Wang, Y. In Situ X-Ray Absorption Fine Structure Studies on the Effect of PH on Pt Electronic Density during Aqueous Phase Reforming of Glycerol. *ACS Catal.* **2012**, *2* (11), 2387–2394. https://doi.org/10.1021/cs3005049.

(23) Esteve-Adell, I.; Crapart, B.; Primo, A.; Serp, P.; Garcia, H. Aqueous Phase Reforming of Glycerol Using Doped Graphenes as Metal-Free Catalysts. *Green Chem.* **2017**, *19* (13), 3061–3068. https://doi.org/10.1039/C7GC01058C.

(24) Katryniok, B.; Paul, S.; Dumeignil, F. Recent Developments in the Field of Catalytic Dehydration of Glycerol to Acrolein. *ACS Catal.* **2013**, *3* (8), 1819–1834. https://doi.org/10.1021/cs400354p.

(25) Zhang, H.; Hu, Z.; Huang, L.; Zhang, H.; Song, K.; Wang, L.; Shi, Z.; Ma, J.; Zhuang, Y.; Shen, W.; et al. Dehydration of Glycerol to Acrolein over Hierarchical ZSM-5 Zeolites: Effects of Mesoporosity and Acidity. *ACS Catal.* **2015**, *5* (4), 2548–2558. https://doi.org/10.1021/cs5019953.

(26) Li, B.; Wang, J.; Yuan, Y.; Ariga, H.; Takakusagi, S.; Asakura, K. Carbon Nanotube-Supported RuFe Bimetallic Nanoparticles as Efficient and Robust Catalysts for Aqueous-Phase Selective Hydrogenolysis of Glycerol to Glycols. *ACS Catal.* **2011**, *1* (11), 1521–1528. https://doi.org/10.1021/cs200386q.

(27) Huang, Z.; Cui, F.; Kang, H.; Chen, J.; Zhang, X.; Xia, C. Highly Dispersed Silica-Supported Copper Nanoparticles Prepared by Precipitation− Gel Method: A Simple but Efficient and Stable Catalyst for Glycerol Hydrogenolysis. *Chem. Mater.* **2008**, *20*, 5090–5099. https://doi.org/doi: 10.1021/cm8006233.

(28) Wang, S.; Liu, H. Selective Hydrogenolysis of Glycerol to Propylene Glycol on Cu–ZnO Catalysts. *Catal. Letters* **2007**, *117* (1–2), 62–67. https://doi.org/10.1007/s10562-007-9106-9.

(29) Dasari, M. A.; Kiatsimkul, P.-P.; Sutterlin, W. R.; Suppes, G. J. Low-Pressure Hydrogenolysis of Glycerol to Propylene Glycol. *Appl. Catal. A Gen.* **2005**, *281* (1–2), 225–231. https://doi.org/10.1016/J.APCATA.2004.11.033.

(30) Guo, L.; Zhou, J.; Mao, J.; Guo, X.; Zhang, S. Supported Cu Catalysts for the Selective Hydrogenolysis of Glycerol to Propanediols. *Appl. Catal. A Gen.* **2009**, *367* (1–2), 93–98. https://doi.org/10.1016/J.APCATA.2009.07.040.

(31) Mane, R. B.; Hengne, A. M.; Ghalwadkar, A. A.; Vijayanand, S.; Mohite, P. H.; Potdar, H. S.; Rode, C. V. Cu:Al Nano Catalyst for Selective Hydrogenolysis of Glycerol to 1,2-Propanediol. *Catal. Letters* **2010**, *135* (1–2), 141–147. https://doi.org/10.1007/s10562-010-0276-5.

(32) Yuan, Z.; Wang, J.; Wang, L.; Xie, W.; Chen, P.; Hou, Z.; Zheng, X. Biodiesel Derived Glycerol Hydrogenolysis to 1,2-Propanediol on Cu/MgO Catalysts. *Bioresour. Technol.*

2010, *101* (18), 7088–7092. https://doi.org/10.1016/J.BIORTECH.2010.04.016.

(33) Akiyama, M.; Sato, S.; Takahashi, R.; Inui, K.; Yokota, M. Dehydration–hydrogenation of Glycerol into 1,2-Propanediol at Ambient Hydrogen Pressure. *Appl. Catal. A Gen.* **2009**, *371* (1–2), 60–66. https://doi.org/10.1016/J.APCATA.2009.09.029.

(34) Nakagawa, Y.; Tomishige, K. Heterogeneous Catalysis of the Glycerol Hydrogenolysis. *Catal. Sci. Technol.* **2011**, *1* (2), 179. https://doi.org/10.1039/c0cy00054j.

(35) Zhu, S.; Gao, X.; Zhu, Y.; Zhu, Y.; Zheng, H.; Li, Y. Promoting Effect of Boron Oxide on Cu/SiO2 Catalyst for Glycerol Hydrogenolysis to 1,2-Propanediol. *J. Catal.* **2013**, *303*, 70–79. https://doi.org/10.1016/J.JCAT.2013.03.018.

(36) Wan, W.; Ammal, S. C.; Lin, Z.; You, K.-E.; Heyden, A.; Chen, J. G. Controlling Reaction Pathways of Selective C–O Bond Cleavage of Glycerol. *Nat. Commun.* **2018**, *9* (1), 4612. https://doi.org/10.1038/s41467-018-07047-7.

(37) Skoplyak, O.; Barteau, M. A.; Chen, J. G. Enhancing H2 and CO Production from Glycerol Using Bimetallic Surfaces. *ChemSusChem* **2008**, *1* (6), 524–526. https://doi.org/10.1002/cssc.200800053.

(38) Hwu, H. H.; Chen, J. G. Reactions of Methanol and Water over Carbide-Modified Mo(1 1 0). *Surf. Sci.* **2003**, *536* (1–3), 75–87. https://doi.org/10.1016/S0039-6028(03)00607-1.

(39) Frühberger, B.; Chen, J. G. Reaction of Ethylene with Clean and Carbide-Modified Mo(110): Converting Surface Reactivities of Molybdenum to Pt-Group Metals. *J. Am. Chem. Soc.* **1996**, *118* (46), 11599–11609. https://doi.org/10.1021/ja960656l.

(40) Yu, W.; Salciccioli, M.; Xiong, K.; Barteau, M. A.; Vlachos, D. G.; Chen, J. G. Theoretical and Experimental Studies of C-C versus C-O Bond Scission of Ethylene Glycol Reaction Pathways via Metal-Modified Molybdenum Carbides. *ACS Catal.* **2014**,

4 (5), 1409–1418. https://doi.org/10.1021/cs500124n.

(41) Ayre, C. R.; Madix, R. J. The Adsorption and Reaction of 1,2-Propandiol on Ag (110) under Oxygen Lean Conditions. *Surf. Sci.* **1994**, *303*, 279–296. https://doi.org/10.1016/0039-6028(94)90776-5.

SYNOPSIS

1,2-propanediol was shown to be a surrogate with higher vapor pressure and simpler structure for glycerol gas-phase mechanistic studies.

Table of content